Volume 52 • Number 23
December 2017

Journal of Materials Science

jMS

10853 • 52(23) 13319–13684 (2017)
ISSN 0022-2461 (Print)
ISSN 1573-4803 (Electronic)

Springer

J Mater Sci (2017) 52:13455–13465

Chemical routes to materials

Efficient in situ growth of platinum nanoclusters on the surface of Fe_3O_4 for the detection of latent fingermarks

Rui Huang[1,*] and Rui Liu[1,2]

[1] Chongqing Institution of Higher Learning Center of Forensic Science Engineering and Research, Southwest University of Political Science and Law, Chongqing 401120, China
[2] Criminal Investigation College of Southwest University of Political Science and Law, Chongqing 401120, China

Received: 17 May 2017
Accepted: 14 August 2017
Published online: 23 August 2017

ABSTRACT

Hydrophobic Fe_3O_4 nanoparticles were modified with polyethyleneimine (PEI) to obtain hydrophilic Fe_3O_4 nanoparticles. By reducing the content of H_2PtCl_6 solution by using L-ascorbic acid (AA) as a reductive agent, fluorescent platinum nanoclusters (Pt NCs) were incubated into the PEI-modified Fe_3O_4 nanoparticles. The prepared Fe_3O_4@Pt NCs microspheres possessed a uniform size, improved monodispersity, high magnetization (40.8 emu/g) and high fluorescence quantum yield (9.0%). Moreover, compared to the reported methods, this method demonstrated that the incubation of Pt NCs on the surface of PEI-Fe_3O_4 was more convenient and needed less reaction time (about 10 min). The experimental results showed that latent fingermarks developing with Fe_3O_4@Pt NCs powder exhibit excellent ridge details. The Fe_3O_4@Pt NCs with superparamagnetism and excellent fluorescence showed great potential in forensic science.

Introduction

Fe_3O_4 nanomaterial shows great potential in sensors, immunoassay and bio-imaging because of excellent permeability and unique superparamagnetism [1, 2]. However, there are many factors to limit its application, such as simple function, aggregation and precipitation [3]. Fluorescent metal nanoclusters, aggregated from several to several tens of metal atoms, have been studied and applied in biological imaging [4], optoelectronics [5] and forensic science [6] due to their excellent physicochemical property. Among these, Pt NCs have been widely studied for excellent catalytic performance [7] and optical property [8]. But the requirement of the small size of fluorescent metal nanoclusters contributes to the limitation of their application. Compared to individual single-component materials, the core–shell nanocomposite containing two or more kinds of materials can exhibit novel physical and chemical

Address correspondence to E-mail: 36287891@qq.com

DOI 10.1007/s10853-017-1475-x

properties. Thus, it is paid great interest in nanomaterial field. For example, the nanocomposite containing Fe_3O_4 and noble metal nanomaterials is the most favored candidate [9, 10].

As the most reliable evidence in forensic science, fingermarks can remain unchanged during one's lifetime and can be used to distinguish a person from others [11]. The latent fingermark, which is presented but invisible at a crime scene, is the most common form of evidence in identification and generalized proof of identity [12]. To visualize latent fingermarks, the application of physical or chemical techniques is required [13]. With the development of fingermarks for hundreds of years, a series of methods have been established, such as "502" glue smoke revealing [14], ninhydrin [15] and DFO [16]. Magnetic Fe_3O_4, widely used in practice, can detect latent fingermarks on different light-colored objects. But detection results are not satisfied when the surface is dark [3]. Therefore, fluorescent nanomaterials such as quantum dots (QDs) and rare earth upconversion fluorescent nanomaterials (UCNMs) have been considered as new agents for the detection of latent fingermarks due to their excellent optical property. For example, Wang et al. have first employed lysozyme-binding aptamer (LBA)-modified NaYF4:Yb, Er UCNMs and CdTe QDs in the detection of latent fingermarks on marbles. The marbles treated with LBL-CdTe QDs show no fingermark but strong purple background fluorescence under the excitation of 365 nm UV light. However, there is no background fluorescence when the fingermarks are treated with LBL-NaYF4:Yb, Er UCNMs under the excitation of 980 nm NIR lights. This strategy can further serve as a robust approach to the detection of latent fingermarks, but a relatively longtime of 30 min for incubation is required [17]. Besides, CdSe QDs [18], semiconducting polymer dots [19] and $SiO_2@Y_2O_3:Eu^{3+}, Li^+$ [20] have also been applied in the detection of latent fingermarks. However, there are many reasons to limit their application, such as complex preparation process, potential toxicity and radioactivity. In previous study, Pt NCs synthesized by bovine serum albumin (BSA), which is non-toxic, have been successfully applied in the development of latent fingermarks [21]. But the small size of particles of BSA-Pt NCs makes it easy to fall into the furrows of fingermarks, weakening the detection of latent fingermarks.

In this work, in situ *growth* method of fluorescent nanoclusters on the surface of magnetic nanomaterials is proposed. Branched PEI is used to modify hydrophobic Fe_3O_4 to obtain hydrophilic Fe_3O_4 nanoparticles. Then, fluorescent Pt NCs are incubated into PEI-modified Fe_3O_4 nanoparticles by reducing the content of H_2PtCl_6 solution and taking AA as a reductive agent in only 10 min. The prepared Fe_3O_4@Pt NCs core–shell microspheres maintain the fluorescence of the particles and possess a uniform size, improved monodispersity and non-toxic. When it comes to the application of fingermark detection, the superparamagnetism of Fe_3O_4 provides the effect of bonding with latent fingermarks by magnetic field force. Meanwhile, Pt NCs play a role of bonding with the organic groups in fingermarks. Compared with traditional fluorescent powder fingermark agents, Fe_3O_4@Pt NCs core–shell microspheres with superparamagnetism and excellent fluorescence can combine with latent fingermarks and emit orange–red fluorescence. This is a potential usage in a broader range of application.

Experimental

Materials and methods

Chloroplatinic acid (H_2PtCl_6) was purchased from Guangfu (Tianjin Guangfu Fine Chemical Research Institute, China). Glutathione (GSH) was purchased from Hongrui (Hongrui Biotechnology Co. Ltd., China). Ascorbic acid (AA), branched polyethyleneimine (PEI, Mn = 10000), ferrous sulfate ($FeSO_4 \cdot 7H_2O$) and ferric chloride ($FeCl_3 \cdot 6H_2O$) were purchased from Sinopharm (Sinopharm Chemical Reagent Co. Ltd., China). All chemicals and solvents employed were of analytical grade. Microwave oven (Glanz, P70D20TJ-D3) and ultra-centrifugation (Shanghai Jing Hong laboratory equipment Corporation, JP-040) were used for synthesis. UV–Vis spectrophotometer (Shimadzu Corporation, UV-2450), fluorescence spectrometer (Shimadzu Corporation, RF-5301PC), particle size and zeta potential analyzer (Bruker, ZetaPALS), scanning electron microscope (JEOL, JSM649OLV) and transmission electron microscope (Philips, TECNAT-10) were used for the characterization and the optimization of Fe_3O_4@Pt NCs. Other devices included ultra-pure water machine (Millipore, Milli-Q) and analytical balance (Shenyang Longteng Electronic Corporation, ESJ200-4B).

The synthesis of Fe_3O_4 nanoparticles

Fe_3O_4 nanoparticles were synthesized through co-precipitation [22]. $FeSO_4 \cdot 7H_2O$ (0.64 M) and $FeCl_3 \cdot 6H_2O$ (1.28 M) were added into a three-necked flask. After mixed evenly, the solution was given 2 mL NaOH solution (1.0 M) under vigorous magnetic stirring for over 30 min. The pH of the mixture was up to 12. The particles were then centrifuged for 15 min at 10000 rpm. Subsequently, the obtained supernatant solution was discarded, and then, the precipitate was washed with deionized water. Washing procedure was performed three times. The magnetic nanoparticles were transferred to a vacuum oven and dried at 60 °C for 8 h to prepare dark brown Fe_3O_4 nanoparticle powder.

The modification of Fe_3O_4 nanoparticles

In 200 mL PEI (20%) solution, 3.70 g Fe_3O_4 nanoparticle powder was dissolved under stirring at 80 °C. The mixture was put in a microwave oven (power 800 W) with microwave radiation for 30 s and then was centrifuged through ultra-centrifugation for nearly 2 h. After separation, the precipitate was washed with deionized water to neutral and then was dried to obtain Fe_3O_4 particles modified by PEI.

In situ *growth* of Pt NCs on Fe_3O_4 nanoparticles

The prepared PEI-Fe_3O_4 and H_2PtCl_6 solution (0.01 mL, 1 g in 100 mL) was dispersed in 8 mL of ultra-pure water under stirring. After stirred for 5 min, AA solution (0.1 M) was added into the mixed solution. Moreover, GSH solution (0.1 M) was added into the solution after another 5 min. Then, the color of the solution was obviously deepened to obtain Fe_3O_4@Pt NCs core–shell microspheres.

The characterization of Fe_3O_4@Pt NCs

The morphology of Fe_3O_4@Pt NCs was measured by means of SEM and TEM. Particle size was determined by zeta potential analyzer. The XRD spectrums of samples were acquired from 10° to 80°, which was employed to confirm the successful synthesis of Pt NCs on the surface of Fe_3O_4. The magnetic property was measured by means of VSM. The fluorescence spectrums of samples were performed on fluorescence spectrometer with the scanning range from 510 to 740 nm. In addition, the quantum yield of Fe_3O_4@Pt NCs was measured.

The development of latent fingermarks

All fingermarks were provided by the same volunteers whose fingers rubbed on their noses and foreheads. After washing hands, the volunteer marked fingermarks on various surfaces to obtain samples. To simulate crime scenes, the samples were naturally stored in clean trays at moderate intervals. The development of fingermarks was carried out through brushing along the ridge at clockwise direction with Fe_3O_4@Pt NCs powder.

Results and discussion

The synthesis of Fe_3O_4@Pt NCs

There is a three-dimensional space structure like "branch twig" on the surface of Fe_3O_4 after the modification of PEI. Then, H_2PtCl_6 is added into the structure under stirring. A small number of Pt^{4+} will be immobilized into the "branch twig" as base points for in situ *growth*. Pt^{4+} in liquid phase gradually is accumulated to form fluorescent platinum nanoclusters at the base points under the reduction of AA. While platinum nanoclusters grow, a small number of GSHs are used as auxiliary protective agent. What's more, it is also attached to the surface of Fe_3O_4 by the combination with the outermost metal atoms to prevent the gathering of the outermost platinum atoms (Fig. 1). Surprisingly, the incubation time of Pt NCs is just 10 min, much shorter than that of PEI-protected high-luminescent Pt nanoclusters reported by Xu et al. (~1 h) [23]. Moreover, compared with the Fe_3O_4@AuNCs nanocomposites composed of Fe_3O_4 coated with cetyltrimethyl ammonium bromide and GSH-AuNCs by electrostatic attraction reported by Wang et al. [24], the composite material constructed through in situ *growth* costs less time and seems more stable and reliable.

The characterization of Fe_3O_4@Pt NCs

The morphology and the structure of as-prepared samples are characterized. As shown in Fig. 2a, Fe_3O_4

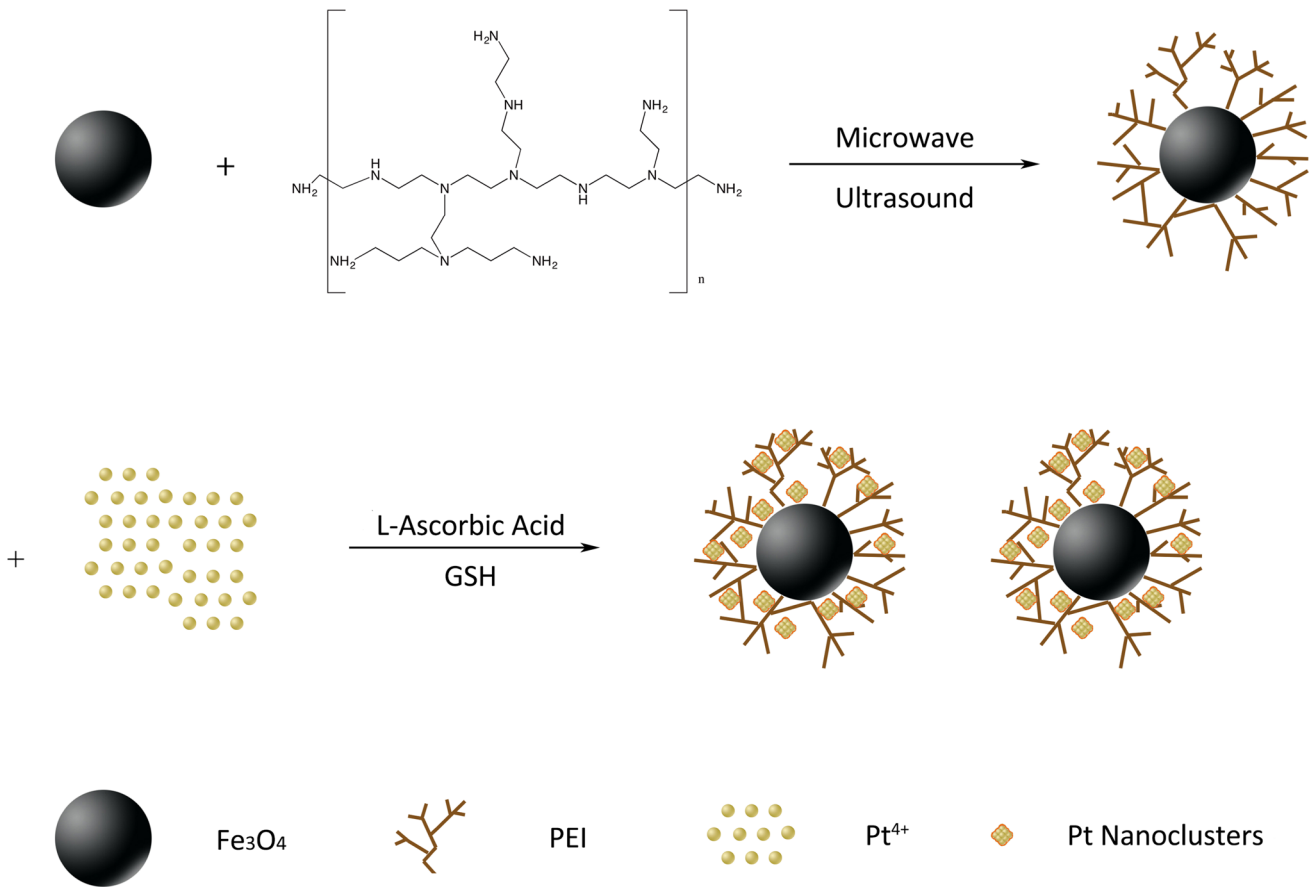

Figure 1 Preparation process diagram of Fe_3O_4@Pt NCs.

nanoparticles are easily aggregated. PEI-Fe_3O_4 (Fig. 2b) is well dispersed for the positive affection of PEI and has a uniform size of average 156 nm smaller than Fe_3O_4 modified with mercapto silane reported by Zhang et al. (~220 nm) [3]. In Fig. 2c, the Fe_3O_4@Pt NCs core–shell microspheres exhibit excellent dispersibility and possess an average particle size of 161 nm larger than that (156 nm) of PEI-Fe_3O_4. This indicates that core–shell nanoparticles are synthesized by the reduction of H_2PtCl_6 with AA on the surface of Fe_3O_4. The particle size of Fe_3O_4@Pt NCs is further measured by zeta potential analyzer. The result shows that the particle size of Fe_3O_4@Pt NCs is about 159 nm (Fig. 2d), which matches the result by electron microscopy.

To further validate the successful synthesis of Fe_3O_4@Pt NCs, the crystal structure of the samples is checked by the XRD pattern shown in Fig. 3. The XRD spectrum of PEI-Fe_3O_4 in Fig. 3a shows diffraction peaks at 30°, 34.9°, 44.2°, 57.2° and 64.1°, which well match with those of JCPDS card [25]. The XRD pattern of Fe_3O_4@Pt NCs in Fig. 3b reserves the Bragg's reflection of Fe_3O_4 on (220), (311), (400) and (440), which may be caused by the formation of Pt NCs shells on the surface of Fe_3O_4. At the same time, the XRD curve of Fe_3O_4@Pt NCs has a wide characteristic peak in the range from 10° to 25°, which may be related to the amorphous structure of Pt NCs [26]. The weakening and the disappearance of the diffraction peaks of Fe_3O_4 and the expression of the amorphous structure of Pt NCs confirm the successful incubation of Pt NCs on the surface of Fe_3O_4 and the core–shell microspheres encapsulated by Pt NCs outside Fe_3O_4.

Magnetic property is of importance in the practice of the detection of latent fingermarks. Figure 4 presents the magnetization curve of Fe_3O_4@Pt NCs. The M (H) hysteresis curve for PEI-Fe_3O_4 nanoparticles in Fig. 4a is reversible, which suggests a superparamagnetic characteristic [27]. The magnetization curve

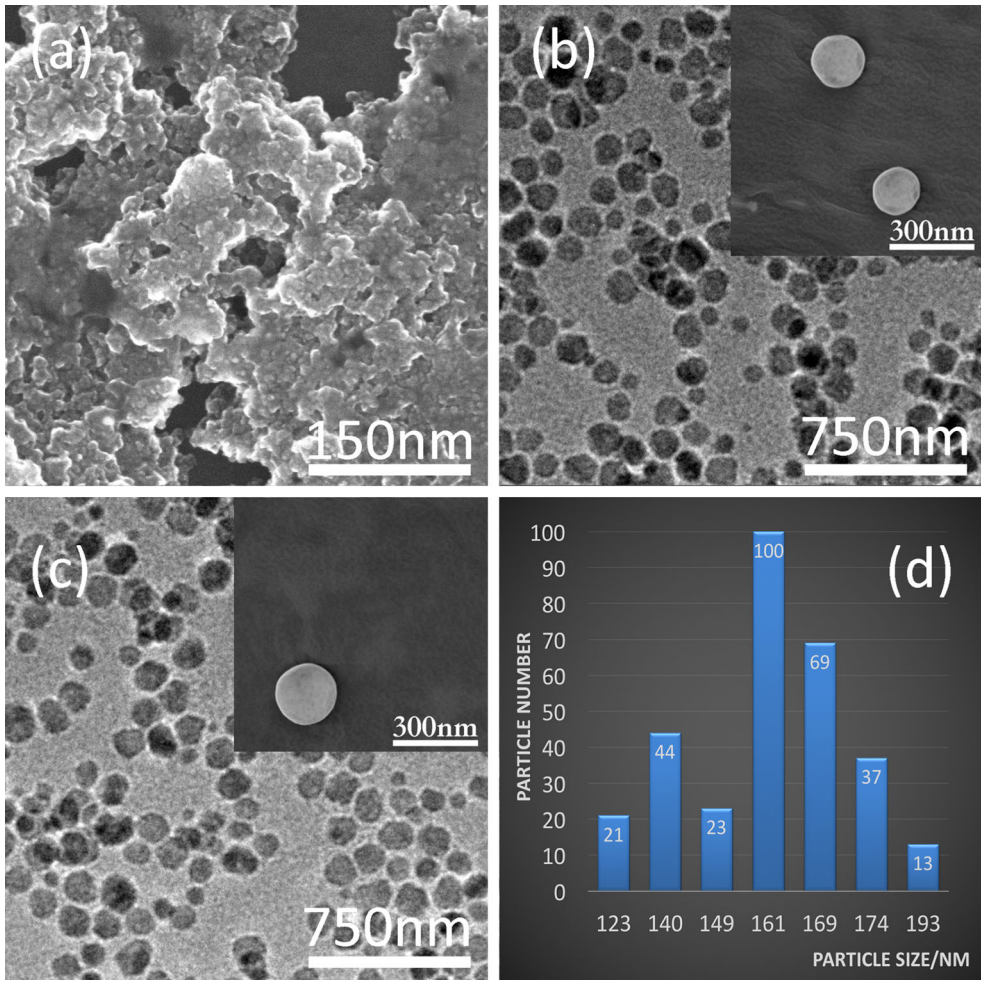

Figure 2 **a** SEM image of Fe_3O_4, **b** TEM image of PEI-Fe_3O_4, **c** TEM image of Fe_3O_4@Pt NCs and **d** size distribution of Fe_3O_4@Pt NCs. The *inset* displays the SEM image of PEI-Fe_3O_4 and Fe_3O_4@Pt NCs.

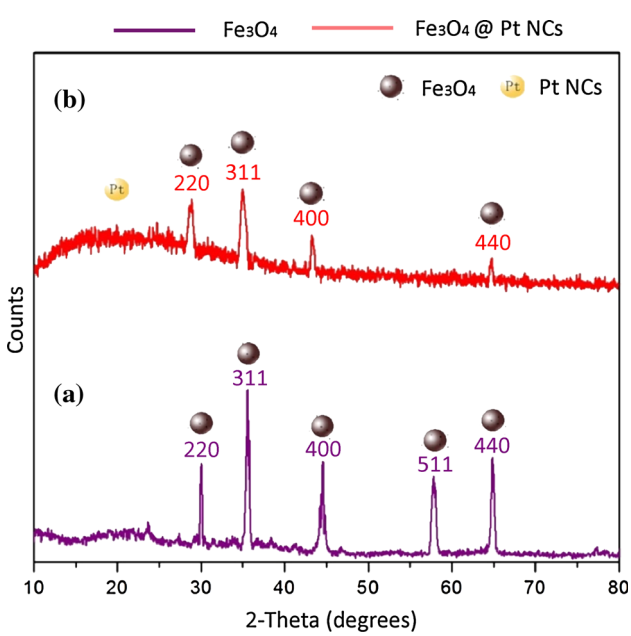

Figure 3 XRD chart of *a* Fe_3O_4 and *b* Fe_3O_4@Pt NCs.

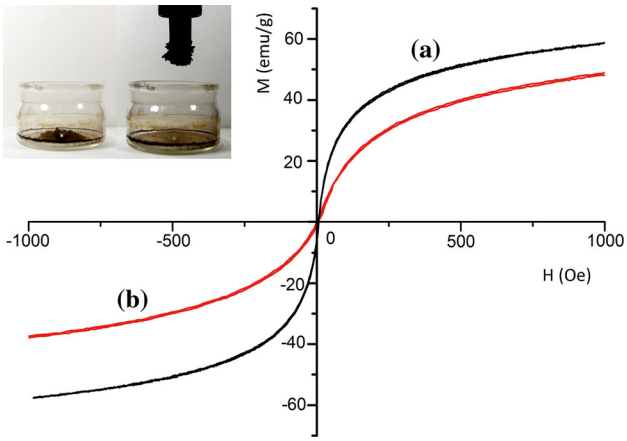

Figure 4 Magnetic chart of *a* Fe_3O_4 and *b* Fe_3O_4@Pt NCs. The *inset* displays the Fe_3O_4@Pt NCs powders absorbed by magnetic brush.

of Fe_3O_4@Pt NCs in Fig. 4b indicates that its magnetic strength (40.8 emu/g) is weaker than that (59.8 emu/g) of PEI-Fe_3O_4 nanoparticles. It implies that the coat

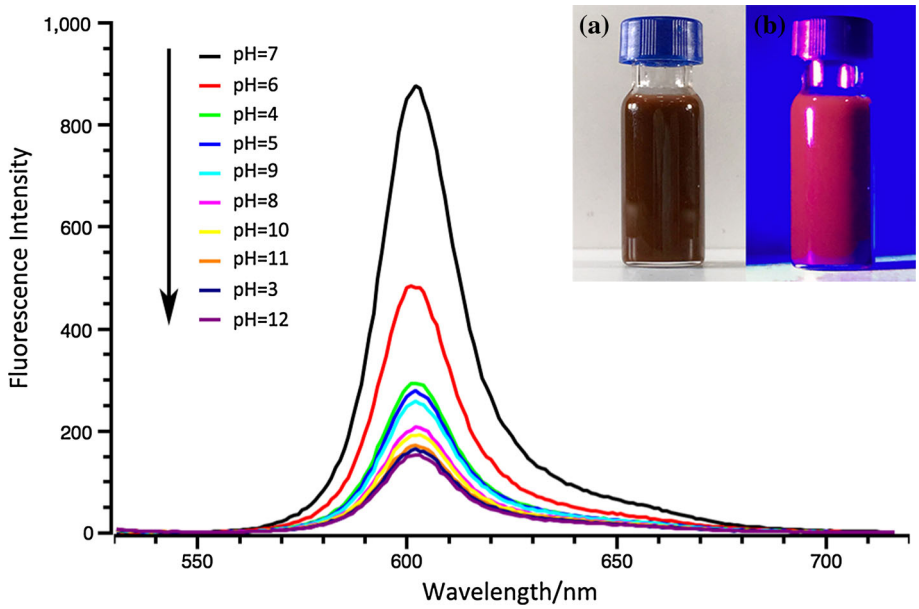

Figure 5 Fluorescence spectrum and the *inset* is the photograph of Fe_3O_4@Pt NCs under *a* normal fluorescent indoor lighting or *b* 415 nm light.

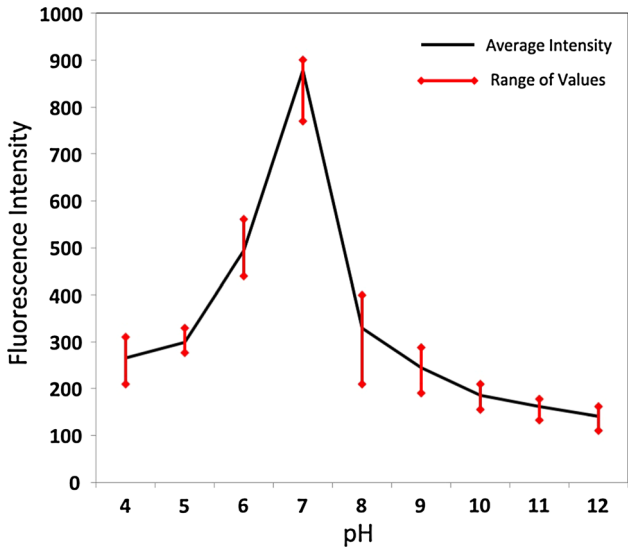

Figure 6 Fe_3O_4@Pt NCs under different pH conditions were prepared five times and their fluorescence intensity was performed.

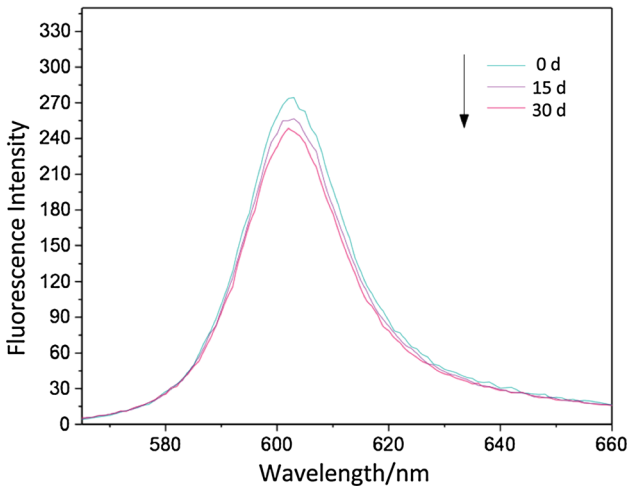

Figure 7 Fluorescence intensity changes of Fe_3O_4@Pt NCs in a month (under about 25 °C and 30% humidity).

of Pt NCs on the surface of PEI-Fe_3O_4 weakens saturation magnetization to some extent. But the magnetic strength of Fe_3O_4@Pt NCs is still higher than that of the Fe_3O_4@SiO_2-Au (for 0.4 emu/g) reported by Li et al. [28]. Among the five samples of Fe_3O_4@Pt NCs constructed in the same conditions, their RSD is <4.8%. Figure 4 displays the Fe_3O_4@Pt NCs powder absorbed by magnetic brush. The magnetic property of Fe_3O_4@Pt NCs contributes to its application in the detection of latent fingermarks.

Fluorescence intensity greatly influences the effect of fingermark detection. The prepared PEI-Fe_3O_4 is centrifuged by ultra-centrifugation. After separation, the precipitate is washed with deionized water to neutral. Then, Pt NCs are incubated by AA on the surface of PEI-Fe_3O_4 under different pH conditions adjusted by HCl and NaOH. The emission spectra of Fe_3O_4@Pt NCs under different pH conditions are shown in Fig. 5. They indicate that fluorescence intensity increases with increasing pH increasing from 3 to 7 and decreases with pH decreasing from 7 to 12. This may be due to the destruction of the

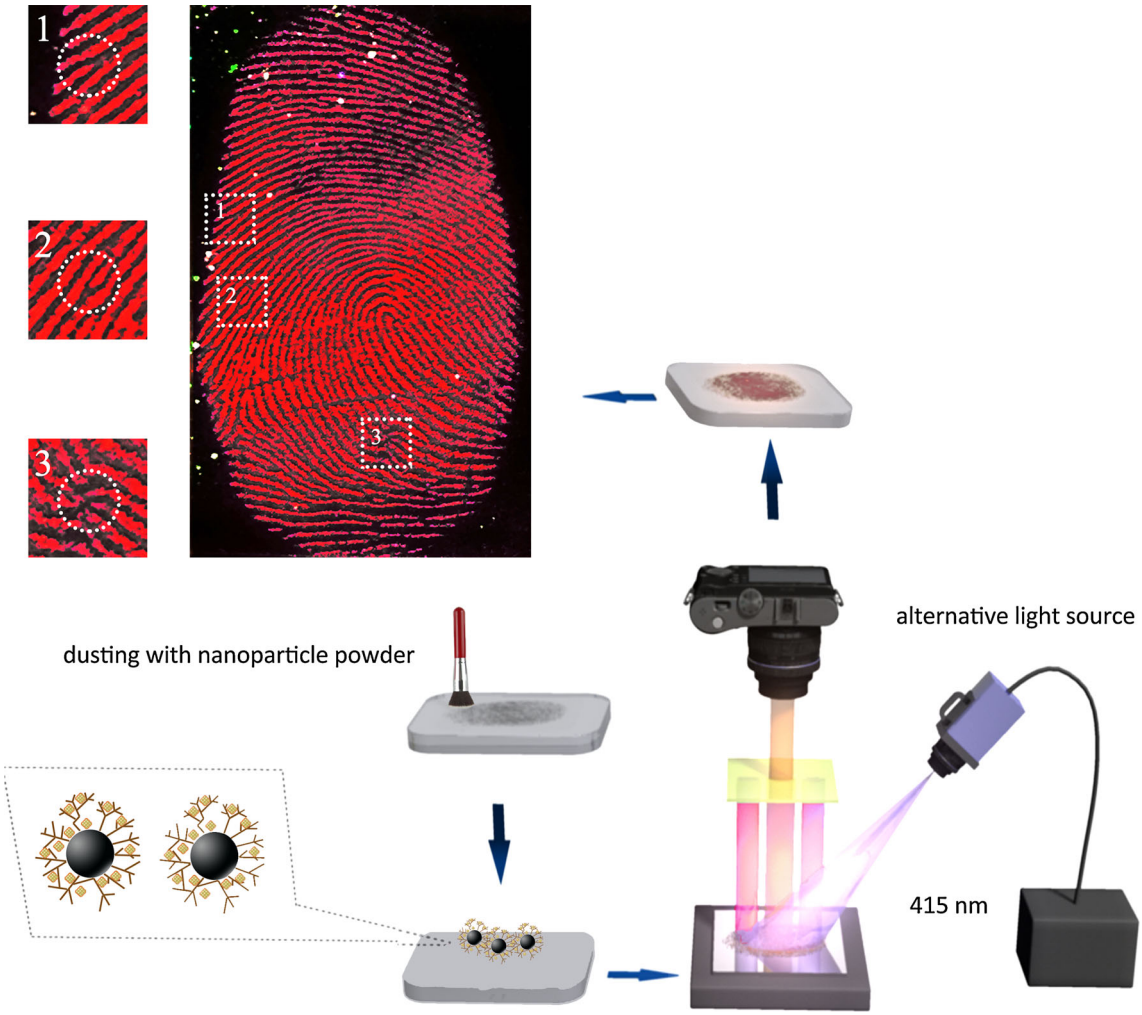

Figure 8 Development principle of Fe_3O_4@Pt NCs powders with self-assembly development observation system: fingermarks developed on glass surface using Fe_3O_4@Pt NCs powders showing detail features: *1* termination, *2* origin; *3* scar. The image of detected fingermark was processed by photoshop to enhance brightness and contrast. And the unprocessed figure is visible in Supporting Information (Supplementary Figure 1, S1).

structural property of template PEI under acid or alkali environment. In addition, a decrease in Pt NCs incubated on the surface of Fe_3O_4 needs further research. The quantum yield of Fe_3O_4@Pt NCs synthesized under neutral environment has been further determined by Rhodamine B, as a reference sample [29]. A quantum yield of 9.0% (RSD = 0.4%, $n = 5$) is obtained, slightly lower than that of PEI-Pt NCs (11%) reported by Huang et al. [8]. The fluorescence quenching of Pt NCs may be caused by the presence of Fe_3O_4. However, according to previous study [21], the quantum yield of Fe_3O_4@Pt NCs is sufficient to meet the needs of the detection of latent fingermarks.

To ensure the reliability of experimental results, the samples under different pH are prepared five times, and their fluorescence intensity is performed (Fig. 6). Fluorescence stability is important for promoting a new fingermark detecting agent in practice. Figure 7 shows the change of the fluorescence intensity of Fe_3O_4@Pt NCs for 15 and 30 days when it is stored in shade under the humidity of approximate 25 °C and 30%. As shown in Fig. 7, Fe_3O_4@Pt NCs exhibits excellent fluorescence stability. The fluorescence intensity of Fe_3O_4@Pt NCs maintains more than 91.7 and 89.3% of the initial fluorescence value.

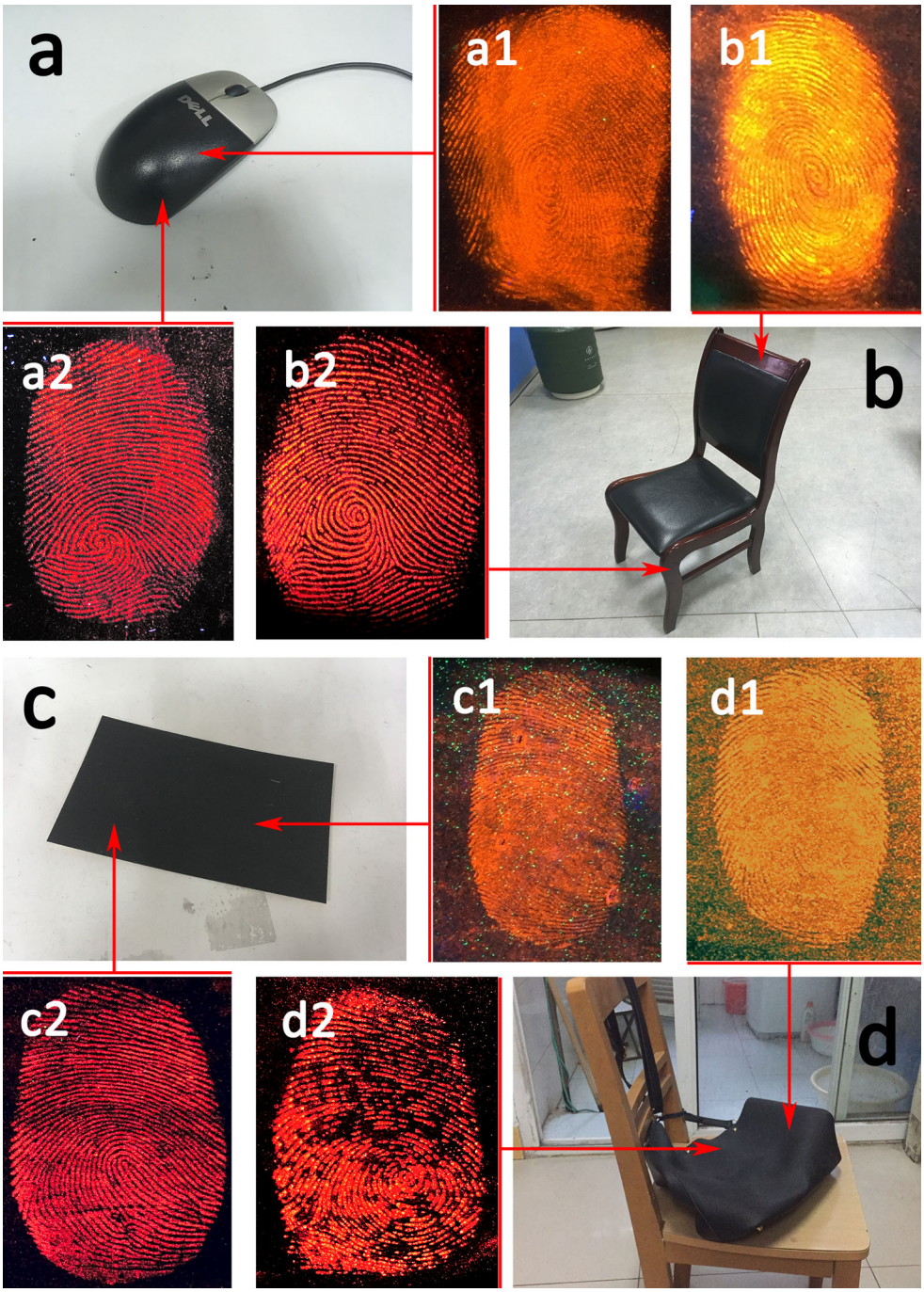

Figure 9 Latent fingermarks on **a** a *black* plastic mouse, **b** a *dark brown* wood stool, **c** a piece of *black* paper and **d** a *black* leather bag were detected by (1) traditional fluorescent powders and (2) Fe_3O_4@Pt NCs. The images of detected fingermarks were processed by photoshop to enhance brightness and contrast. And the unprocessed figure is visible in Supporting Information (Supplementary Figure 2, S2).

The development of Latent Fingermarks

As the most reliable form of evidence in identification, fingermark can provide plenty of valuable information [30]. Sweat pores which can secret large amounts of sweat are widely distributed on the ridge of fingermarks [31]. According to Locard Principle, the latent fingermarks left on surfaces contain many constituents due to the secretions from sebaceous eccrine and apocrine gland such as water, protein and fat.

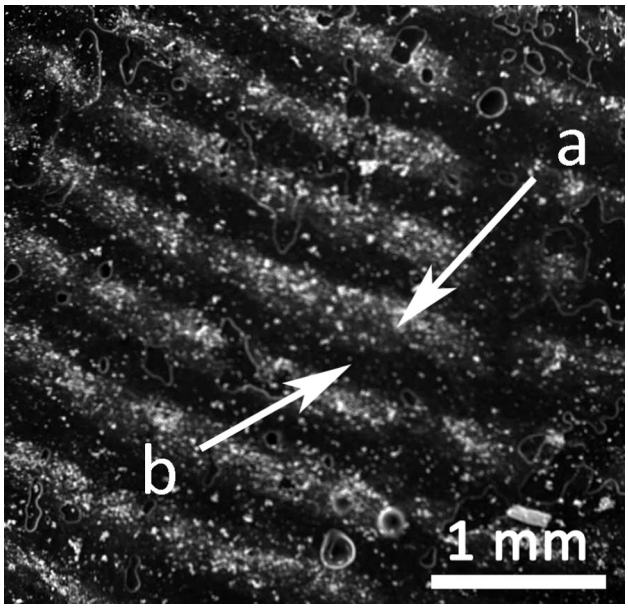

Figure 10 SEM image of latent fingerprint detected by Fe_3O_4@-Pt NCs.

Figure 8 shows a self-assembly development observation system. Fingermark powdering remains the most popular technique for the visualization of fingermarks. When Fe_3O_4@Pt NCs powder is excited by the alternative light source at 415 nm, it can be found that the ridge emits orange–red fluorescence with no background. In addition, first-level details (ridge) and second-level details such as (1) ridge termination, (2) origin and (3) scar of fingermarks are excellently detected. Moreover, the picture also demonstrates the clear interaction between Fe_3O_4@Pt NCs and sebaceous excretion.

Figure 9 shows the sweat latent fingermarks detected by (1) traditional fluorescent powders and (2) Fe_3O_4@Pt NCs on (a) a black plastic mouse, (b) a dark brown wood stool, (c) a piece of black paper and (d) a black leather bag. It can be easily found that the latent fingermarks developing with Fe_3O_4@Pt NCs show excellent ridge details with minimal background staining and better results. Compared with traditional fluorescent powders, the above is due to its nanosize, superparamagnetism and outstanding fluorescence. The above image shows that Fe_3O_4@Pt NCs yields good results on most surfaces except leather surface because of its uneven surface. But it is still clear enough to distinguish the detail features from the detected fingermarks.

The details about fingermarks developing with Fe_3O_4@Pt NCs are characterized by SEM and EDX.

Table 1 EDX spectra of the (region a) ridges and (region b) furrows of latent fingermarks detected by Fe_3O_4@Pt NCs

Element	wt%	at.%
Region a		
C K	7.49	15.61
O K	39.23	61.36
Cl K	1.07	0.76
Fe K	48.69	21.82
Pt L	3.52	0.45
Totals	100.00	
Region b		
C K	69.44	75.90
O K	28.90	23.71
Fe K	1.66	0.39
Totals	100.00	

Figure 10 shows the image of SEM. As shown in Table 1, Fe_3O_4@Pt NCs appears on (region a) the ridges of developed latent fingermarks, while no Fe_3O_4@Pt NCs is presented on (region a) furrows. Therefore, Fe_3O_4@Pt NCs shows good selectivity to the dermal ridge of fingermarks.

Conclusions

In this work, novel composite nanometer core–shell microspheres with superparamagnetism and excellent fluorescence are synthesized by efficient in situ *growth* of Pt NCs on the surface of Fe_3O_4 modified with PEI in just 10 min. Compared with the previous research results from other researchers, the structure and the properties of Fe_3O_4@Pt NCs are characterized by a series of characterization methods. The magnetic strength of composites is 40.8 emu/g, and the fluorescence quantum yield is 9.0%. This paper finds the relationship between the fluorescence of composites and pH values during preparation. The detection result of sweat latent fingermarks on different kinds of objects is excellent, which provides a new and efficient method for the visualization of latent fingermarks. Furthermore, magnetic fluorescent nanomaterials have broad application prospects in more fields. Particularly in the biomedical field, Fe_3O_4@Pt NCs will also play an important role in biological imaging, biological tracers and targeted transport.

Acknowledgements

This work was supported by Foundation and Frontier Research Program of Chongqing Municipal

Science and Technology Commission (cstc2016jcyjA0503, cstc2017jcyjAX0244), Science and Technology Research Project of Chongqing Municipal Education Commission (KJ1500111), Research Program of Chongqing University Forensic Engineering Research Center (LCFS1421), Project Supported by Southwest University of Political Science and Law in 2015 (2015XZON-27) and Student Research and Innovation Project of Southwest University of Political Science and Law in 2016 (2016ZXZS-156).

Compliance with ethical standards

Conflict of interest The authors declare that they have no conflicts of interest.

Electronic supplementary material: The online version of this article (doi:10.1007/s10853-017-1475-x) contains supplementary material, which is available to authorized users.

References

[1] Bakheet AAAA, Zhu XS (2017) Determination of rhodamine b pigment in food samples by ionic liquid coated magnetic core/shell Fe_3O_4@SiO_2 nanoparticles coupled with fluorescence spectrophotometry. Science 5(1):1–7

[2] Qiao L, Fu Z, Li J et al (2017) Standardizing size-and shape-controlled synthesis of monodisperse magnetite (Fe_3O_4) nanocrystals by identifying and exploiting effects of organic impurities. ACS Nano 11(6):6370–6381

[3] Zhang LY, Zhou XF, Chu T (2013) Preparation and evaluation of Fe_3O_4-core@Ag-shell nanoeggs for the development of fingerprints. Sci China Chem 56:551–556. doi:10.1007/s11426-012-4764-x

[4] Kundu N, Mukherjee D, Maiti TK et al (2017) Protein guided formation of silver nano-clusters and its assembly with graphene oxide act as an improved bio-imaging agent with reduced toxicit. J Phys Chem Lett 8(10):2291–2297

[5] Lin HT, Cai KB, Huang HY et al (2017) Thermally-activated delayed fluorescence from biocompatible, solid-state gold nanoclusters embedded into ionic-crystal matrices. J Lumin 187:269–273

[6] Huang R, Chen H, Xia Z (2017) Ultrasonic-microwave heating synthesis and latent fingermarks development of gold nanoclusters. Bull Chem Soc Jpn 90:754–759. doi:10.1246/bcsj.20170016

[7] Liu S, Tian N, Xie AY et al (2016) Electrochemically seed-mediated synthesis of sub-10 nm tetrahexahedral Pt nanocrystals supported on graphene with improved catalytic performance. J Am Chem Soc 138(18):5753–5756

[8] Huang X, Aoki K, Ishitobi H et al (2014) Preparation of Pt nanoclusters with different emission wavelengths and their application in Co^{2+} detection. ChemPhysChem 15(4):642–646

[9] Pardo IR, Roig-Pons M, Heredia AA et al (2017) Fe_3O_4@Au@mSiO_2 as enhancing nano-platform for rose bengal photodynamic activity. Nanoscale 9:10388–10396

[10] Hu Y, Wang R, Wang S et al (2016) Multifunctional Fe_3O_4@Au core/shell nanostars: a unique platform for multimode imaging and photothermal therapy of tumors. Sci Rep 6:1–12

[11] Wang M, Li M, Yu A et al (2017) Fluorescent nanomaterials for the development of latent fingerprints in forensic sciences. Adv Funct Mater 27(14):1606243

[12] Barros HL, Stefani V (2016) A new methodology for the visualization of latent fingermarks on the sticky side of adhesive tapes using novel fluorescent dyes. Forensic Sci Int 263:83–91

[13] Schwarz L (2009) An amino acid model for latent fingerprints on porous surfaces. J Forensic Sci 54(6):1323–1326

[14] Kendall FG, Rehn BW (1983) Rapid method of super glue fuming application for the development of latent fingerprints. J Forensic Sci 28(3):777–780

[15] Wang MC, Luo YP (2013) A comparative study of the use of genipin or ninhydrin in fingerprints development. Forensic Sci Technol 6:33–35

[16] Pounds AC, Phil M, Grigg R et al (1990) The use of 1, 8-diazafluoren-9-one (DFO) for the fluorescent detection of latent fingerprints on paper: a preliminary evaluation. J Forensic Sci 35(1):169–175

[17] Wang J, Wei T, Li X et al (2014) Near-infrared-light-mediated imaging of latent fingerprints based on molecular recognition. Angew Chem 126(6):1642–1646

[18] Wang YF, Yang RQ, Shi ZX et al (2014) The effectiveness of CdSe nanoparticle suspension for developing latent fingermarks. J Saudi Chem Soc 18(1):13–18

[19] Chen YH, Kuo SY, Tsai WK et al (2016) Dual colorimetric and fluorescent imaging of latent fingerprints on both porous and nonporous surfaces with near-infrared fluorescent semiconducting polymer dots. Anal Chem 88(23):11616–11623

[20] Venkatachalaiah KN, Nagabhushana H, Darshan GP et al (2017) Novel and highly efficient red luminescent sensor based SiO_2@Y_2O_3:Eu^{3+}, M^+(M^+= Li, Na, K) composite core–shell fluorescent markers for latent fingerprint recognition, security ink and solid state lightning applications. Sens Actuators B Chem 251:310–325

[21] Huang Rui, Liu Rui (2017) Research on development of latent fingerprint by fluorescent platinum nanoclusters. Forensic Sci Technol 42(1):35–39 **(in Chinese)**

[22] Jian P, Fen Z, Lu L et al (2008) Preparation and characterization of PEG-PEI/Fe_3O_4 nano-magnetic fluid by co-precipitation method. Trans Nonferr Met Soc China 18(2):393–398

[23] Xu N, Li HW, Wu Y (2017) Hydrothermal synthesis of polyethylenimine-protected high luminescent Pt-nanoclusters and their application to the detection of nitroimidazoles. Anal Chim Acta 958:51–58

[24] Wang C, Yao Y, Song Q (2015) Gold nanoclusters decorated with magnetic iron oxide nanoparticles for potential multimodal optical/magnetic resonance imaging. J Mater Chem C 3(23):5910–5917

[25] Zheng B, Zhang M, Xiao D et al (2010) Fast microwave synthesis of Fe_3O_4 and Fe_3O_4/Ag magnetic nanoparticles using Fe^{2+} as precursor. Inorg Mater 46(10):1106–1111

[26] Zhang L, Chen D, Jiang Z et al (2012) Facile syntheses and enhanced electrocatalytic activities of Pt nanocrystals with {*hkk*} high-index surfaces. Nano Res 5(3):181–189

[27] Qi X, Li N, Xu Q et al (2014) Water-soluble Fe_3O_4 superparamagnetic nanocomposites for the removal of low concentration mercury (II) ions from water. RSC Adv 4(88):47643–47648

[28] Li X, Li Q, Li Y et al (2013) Latent fingerprints enhancement using a functional composite of Fe_3O_4@SiO_2–Au. Anal Lett 46(13):2111–2121

[29] Kubin RF, Fletcher AN (1983) Fluorescence quantum yields of some rhodamine dyes. J Lumin 27(4):455–462

[30] Champod C, Lennard CJ, Margot P et al (2016) Fingerprints and other ridge skin impressions. CRC Press, Boca Raton

[31] Moret S, Bécue A, Champod C (2016) Functionalised silicon oxide nanoparticles for fingermark detection. Forensic Sci Int 259:10–18